

Performance Enhancement by Secondary Doping in PEDOT:PSS/Planar-Si Hybrid Solar Cells

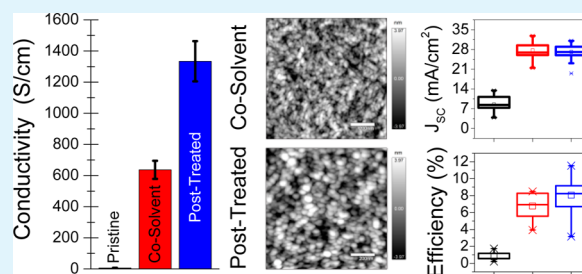
Donald McGillivray, Joseph P. Thomas, Marwa Abd-Ellah, Nina F. Heinig, and K. T. Leung*

WATLab and Department of Chemistry, University of Waterloo, Waterloo, Ontario N2L3G1, Canada

Supporting Information

ABSTRACT: Solar cells depend on effectively absorbing light and converting it into electrical current. It is therefore essential to increase conductivity and to limit both reflection and parasitic absorbance to achieve higher photoconversion efficiency. Here, we examine the effect of post-treatment on the absorbance and conductivity of hybrid solar cells comprised of p-type poly(3,4-ethylene-dioxythiophene) poly(styrenesulfonate) (PEDOT:PSS) on an n-type silicon substrate. Three sets of cells based on pristine PEDOT:PSS film, cosolvent enhanced PEDOT:PSS film using ethylene glycol as a cosolvent, and post-treated PEDOT:PSS film using a novel 1:1 binary mixture of ethylene glycol and methanol have been studied. Markedly different film conductivities have been found for the pristine (~0.8 S/cm), cosolvent added (637 S/cm), and post-treated films (1334 S/cm). The photoconversion efficiency obtained over a large set of samples (72 cells) was used to evaluate the cosolvent addition and post-treatment. Post-treatment is found to reproducibly provide films with not only the highest conductivities but also the highest efficiencies along with higher open-circuit voltage and fill factor but lower short-circuit current density when compared to those of the cosolvent added films. The decrease in the latter is attributed to the increase in absorbance in the PEDOT:PSS film. The present work illustrates the delicate challenge in improving the conductivity and carrier collection efficiency of the cells not at the expense of other properties such as absorption.

KEYWORDS: hybrid solar cells, PEDOT:PSS, secondary doping, post-treatment, external quantum efficiency



INTRODUCTION

Conducting polymers are becoming a viable alternative to inorganic materials used in many devices including different types of solar cells, flexible electronics, and organic energy storage because of their low cost, processability and flexibility. Hybrid solar cells (HSCs) combine these advantages with the high stability, long electron lifetime and long diffusion length of an inorganic material.^{1–8} Single-junction HSCs consisting of an n-type silicon base and a p-type conducting polymer blend [such as poly(3,4-ethylene-dioxythiophene) and poly(styrenesulfonate) (PEDOT:PSS)] emitter have had recently proven photoconversion efficiencies (PCEs) above 14%.^{9,10} They generally have lower processing and manufacturing cost and lower weight than conventional solar cells, providing lower capital cost per watt delivered. They are also highly tunable and can be easily refurbished and reused.

Extensive work has been done to increase the conductivity of the PEDOT:PSS film, and they follow two common approaches: the addition of cosolvents to the aqueous PEDOT:PSS solution used for deposition, and post-treatment of the deposited PEDOT:PSS films. Effective cosolvents include dimethyl sulfoxide (DMSO),^{8,11,12} ethylene glycol (EG),^{13–15} methanol (MeOH),¹⁶ and sorbitol.^{17–19} Enhancement can also be achieved through post-treatment of the films, which involves the removal of PSS and reduction of the film thickness. Unlike with the use of cosolvents, issues with

PEDOT precipitating out of solution can also be avoided in the post-treatment approach. Post-treatment with a single solvent such as EG and MeOH has been used to increase the conductivities to as high as 1418 S/cm²⁰ and 1362 S/cm,²¹ respectively. Both methods can also induce a change in the linear geometry of the PEDOT chains to a more quinoid conformation and consequently a greater delocalization of charges, generally referred as secondary doping.^{13,21,22}

Here, we focus on the important role of conductivity and absorbance of PEDOT:PSS films specifically on the performance of HSCs. We study three sets of films with different conductivities: (a) as-received PEDOT:PSS solution with 0.25 vol % of fluorine surfactant to aid adhesion to silicon (referred here as pristine); (b) cosolvent enhanced PEDOT:PSS solution with 7% EG (cosolvent-added); and (c) cosolvent-added films after a post-treatment with an optimized mixture of two solvents (1:1 volume ratio of MeOH and EG) to increase the conductivity and facilitate the removal of PSS (post-treated).

EXPERIMENTAL DETAILS

The HSCs were prepared on 10 × 10 mm² n-type phosphorus-doped Si(100) substrates with resistivity of 1–2 Ω cm and thickness of 200

Received: August 3, 2016

Accepted: November 14, 2016

Published: November 14, 2016



μm (Virginia Semiconductor Inc.). The substrates were cleaned by sonication sequentially in acetone and isopropyl alcohol and then washed with Millipore water. The native silicon oxide layer on the Si chip was removed with hydrofluoric acid (2 vol %, Sigma-Aldrich) and then exposed to air for 90 min. Aluminum was sputter-coated on the back side of the chip to form the bottom electrode by using a magnetron sputter-coater system (EMS 575X). Pristine films were prepared from a PEDOT:PSS (Clevios PH1000) solution added with a fluorosurfactant (0.25 wt %, Sigma-Aldrich) to increase adhesion to the Si substrate. Cosolvent-added films were prepared from the pristine solution by adding ethylene glycol (7 wt %, VWR, $\geq 99.0\%$) to enhance the conductivity.^{18,23} An aliquot (80 μL) of the PEDOT:PSS solution was spin-coated onto the Si substrate, allowed to relax for 5 min, and then placed on a hot plate at 110 $^{\circ}\text{C}$ for 10 min. Post-treatment was performed by adding an aliquot (80 μL) of a binary mixture of methanol (Sigma-Aldrich, $\geq 99.9\%$) and ethylene glycol with known volume fractions onto the cosolvent-added film. The mixture was drop-casted on and allowed to penetrate the film for 2 min before it was spin-coated at 6000 rpm, allowed to relax for 5 min, and then cured on a hot plate at 110 $^{\circ}\text{C}$ for 10 min. Finally, the top silver electrode was sputter-coated onto the film using a comb-type shadow mask. For optical measurements, the respective PEDOT:PSS films were also prepared separately on $10 \times 10 \text{ mm}^2$ quartz substrates (1 mm thick, SPI Supplies).

Absorbance/transmittance measurements were performed by using a PerkinElmer Lambda 1050 UV-vis-NIR spectrometer. A FilmMetric F40-UV thin film analyzer was used to collect reflectance spectra and determine the film thickness, which was further verified by using a KLA Tencor P6 profilometer. Conductivity measurements were conducted on glass substrates using the four-point probe method in a Van der Pauw configuration (Ecopia HMS-5300). Raman spectra were collected by using a Bruker Senterra dispersive Raman confocal microscope with a 785 nm laser. Atomic force microscopy (AFM) images were obtained by using an Asylum Research Cypher microscope in bimodal AM/FM mode.²⁴ EQE measurements were performed by using a PV Measurements QEX10 system. The solar cells were tested with a $4 \times 4 \text{ cm}^2$ illumination area under 1 Sun condition (100 mW/cm^2) using a PV Measurements IVS solar simulator (equipped with an AM 1.5G filter).

RESULTS AND DISCUSSION

In the present work, we examine the use of MeOH-EG binary mixtures to optimize the post-treatment with these solvents. UV-vis and reflectance measurements were conducted before and after the post-treatment to determine the extent of PSS removal and the reduction in the film thickness, respectively (Figure 1a). The removal of PSS from PEDOT:PSS films can be monitored by the intensity reduction of the absorption band at 193 nm associated with the benzene rings of PSS (Figure S1, Supporting Information).^{11,17} The greatest reductions in the film thickness and PSS absorption band intensity have been found for films post-treated with a 1:1 MeOH-EG mixture. The conductivity was also examined and found to be greatly enhanced with the addition of cosolvent to 637 S/cm and further by over a factor of 2 after post-treatment. Evidently, post-treatment using the MeOH-EG binary mixture leads to the film conductivity enhancement that follows a similar trend as the UV-vis absorption and film thickness with the highest recorded value of 1431 S/cm ($1334 \pm 129 \text{ S/cm}$) found for the 1:1 mixture (Figure 1b). A considerable increase in the conductivity by at least 10% relative to those of single-solvent post-treatment can therefore be obtained by the post-treatment using the 1:1 binary mixture. Experiments with consecutive post-treatment cycles on the same film were attempted. The second cycle would reduce the film thickness by $\sim 10\%$, and repeated cycles produced only insignificant decreases. As the

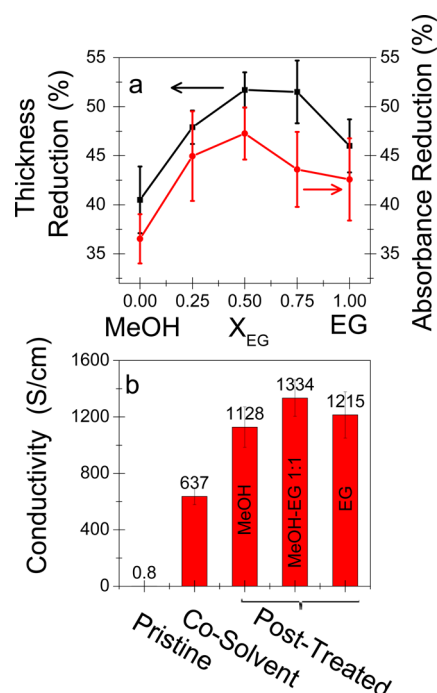


Figure 1. (a) Percent intensity reduction of the PSS absorption band at 195 nm (right) and the percent reduction of film thickness (left) for MeOH-EG solutions with different MeOH:EG ratios. (b) Comparison of conductivities of the pristine, cosolvent-added, and post-treated PEDOT:PSS films.

conductivity did not improve greatly with the subsequent treatments, only one post-treatment cycle was used.

Raman spectroscopy is very sensitive to structural changes in polymers and is useful in studying secondary doping in conjugated polymers.²⁵ The vibrational modes of PEDOT and PSS were followed using a 785 nm excitation line for pristine, cosolvent-added, and post-treated films (Figure 2). The most

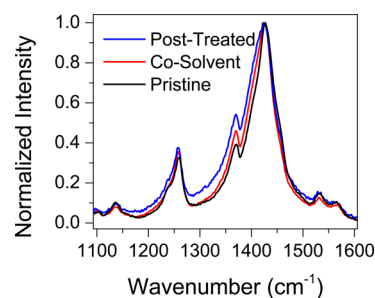


Figure 2. Raman spectra showing the structural changes of PEDOT to a more quinoidal conformation with post-treatment.

intense band located at 1425 cm^{-1} , to which the spectrum is normalized, is assigned to $C_{\alpha}=C_{\beta}$ symmetric stretching, while the two weaker bands at 1532 and 1563 cm^{-1} correspond to the $C_{\alpha}=C_{\beta}$ asymmetric stretching.²⁶ The bands at 1368 and 1256 cm^{-1} are attributed to $C_{\beta}-C_{\beta}$ stretching and $C_{\alpha}-C_{\alpha}$ inter-ring stretching, respectively.²⁵ Broadening of the 1425 cm^{-1} band is evident with the addition of cosolvent, and further broadening is found with post-treatment. The relative intensity of the 1368 cm^{-1} band increases with the addition of a cosolvent and then again with post-treatment. We also observe a slight intensity increase and a red shift for the $C_{\alpha}-C_{\alpha}$ inter-ring stretching at 1256 cm^{-1} . These changes are often

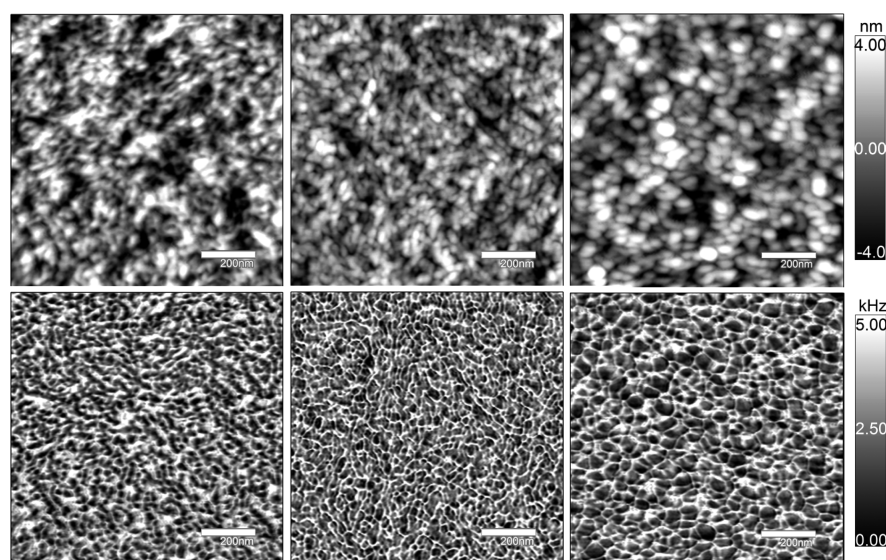


Figure 3. AFM images (topography: top row, with an intensity scale of -4 to 4 nm; frequency: bottom row, with an intensity scale of 0 – 5 kHz; both $1 \times 1 \mu\text{m}^2$) of pristine (left column), cosolvent-added (middle column), and post-treated films (right column) showing the segregation of PEDOT and PSS with secondary doping and the formation of networks (PSS) and nanodomains (PEDOT).

associated with a change in linear structural arrangement from the benzoidal conformation to a more quinoidal-like conformation.²⁵ Although the post-treatment methods are unlikely to provide any additional charge carriers, the change in structural arrangement leads to electronic redistribution, increased charge delocalization, and higher conductivity.^{11,15,22}

High-dielectric solvents such as MeOH and EG could cause phase segregation between PEDOT and PSS due to a reduction in their Coulombic attraction with each other, as reported elsewhere.^{20,21} The reduced attraction and the increased free volume resulting from swelling enable rearrangement of the PEDOT segments into a more linear, quinoid conformation, as confirmed by Raman spectroscopy.^{13,17,27,28} The deviation from ideal behavior with a 1:1 MeOH-EG mixture, as observed with thickness measurements, UV-vis spectroscopy, and Raman spectroscopy, is the result of viscosity lower than that of pure EG and of dielectric constant and charge screening ability higher than those of pure MeOH (Table S1, Supporting Information).²⁹ The MeOH-EG mixture can easily penetrate the PEDOT:PSS film and cause it to swell. It readily interacts through hydrogen bonding with the sulfate group of PSS or with the oxygen atoms of the PEDOT monomer. The charge screening effect between PEDOT and PSS reduces the interchain interaction and the activation barrier for the reorientation of PEDOT chains. The binary mixture has been shown to form a nearly regular solution at $\sim 1:1$ MeOH:EG at room temperature,³⁰ as is commonly found when alcohols are dissolved in nonpolar solvents. This mixture is, however, less stable with possible partial clustering.³¹ The nonzero enthalpy of mixing is expected to increase the segregation between PEDOT and PSS and to further promote chain reorientation. Unlike PEDOT, PSS is soluble in the mixture, and the chains that are not entangled in the matrix can be readily removed with the excess binary solution. For the remainder of this study, we will focus on the post-treated films obtained with the 1:1 MeOH:EG binary mixture.

A morphological change is also observed for PEDOT:PSS films obtained with the cosolvent addition or post-treatment. In the AFM images shown in Figure 3, the respective surface

roughness is seen to increase with average RMS values of 0.96 ± 0.08 , 1.56 ± 0.18 , and 1.81 ± 0.24 nm for pristine, cosolvent-added, and post-treated films, respectively. At the same time, there are emerging domains consisting of paracrystalline PEDOT centers surrounded by PSS. This arrangement is especially evident in the frequency images, which are much more surface sensitive to the softer PSS (bright network) than the harder PEDOT (dark domains).²⁴ The domains become larger and less elongated with the addition of cosolvents and even more so with the post-treatment. The average area of the domains increases from 21.9 to 35.2 to 183 nm², while the aspect ratio increases from 0.308 to 0.312 to 0.428 for pristine to cosolvent-added to post-treated films, respectively.

A collection of 72 HSCs has been constructed, and their performance data were analyzed to provide relevant comparison between treatments shown in Figure 4. Evidently, the V_{OC}

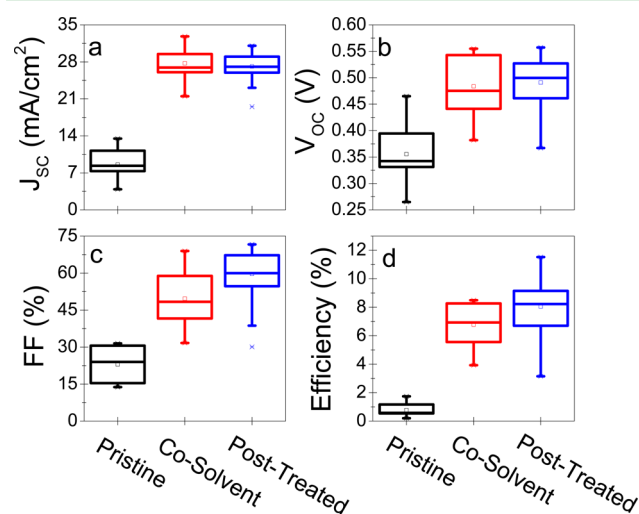


Figure 4. Box plots for (a) short-circuit current density J_{SC} , (b) open-circuit voltage V_{OC} , (c) fill factor FF, and (d) photoconversion efficiency for the 72 hybrid solar cells obtained with pristine, cosolvent-added, and post-treated PEDOT:PSS films.

(Figure 4b) for the cells with post-treated PEDOT:PSS films (average 0.49 V) is found to be slightly higher and with a smaller distribution than those for the cells with cosolvent-added films (0.48 V) and pristine films (0.35 V). The fill factor (Figure 4c) is also consistently higher after post-treatment. The swelling and chain rearrangement during post-treatment allows for the reduction of defects in the film and at the PEDOT:PSS/n-Si interface. This leads to greater charge transfer across the junction and the observed generally larger V_{OC} and fill factor.

The removal of PSS and the enhanced conductivity with post-treatment are expected to have a positive effect on the short-circuit current density, as reported in other devices.^{11,19,21,22} Interestingly, careful examination shows this not to be the case for our HSCs (Figure 4a). The average J_{SC} are 8.58, 27.73, and 27.15 mA/cm² for HSCs with pristine, cosolvent-added, and post-treated films, respectively. To further investigate this unexpected result, external quantum efficiency (EQE) measurements were performed on the HSCs and used to determine J_{SC} . As EQE corresponds to the number of electrons collected per incident photon entering the device,^{1,32–34} EQE measurements can reveal the optical origins of the electronic process occurring in the cell, allowing the determination of a more accurate and reproducible value for J_{SC} .³³ The EQE curves for HSCs with the pristine, cosolvent-added, and post-treated films (85 nm thick) are shown in Figure 5. The EQE curves for HSCs with the pristine and

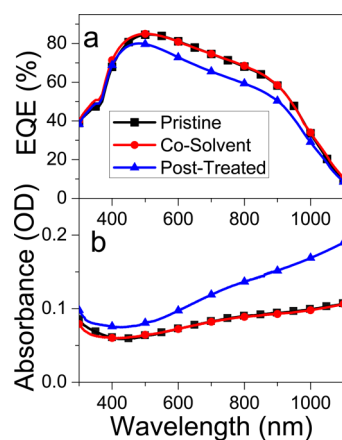


Figure 5. (a) EQE spectra of hybrid solar cells with 85 nm-thick pristine, cosolvent-added, and post-treated PEDOT:PSS films, and (b) absorption spectra of the respective PEDOT:PSS films deposited on quartz substrates.

cosolvent-added films are similar, while that with the post-treated film is discernibly lower. Their corresponding calculated J_{SC} for HSCs with the pristine, cosolvent-added, and post-treated films are 28.2, 28.4, and 25.5 mA/cm², respectively. The lower EQEs for the HSCs with the post-treated films are the result of increased absorbance in the visible and near IR region, as shown in Figure 5b. Increased absorbance in the IR region is attributed to free charge carrier absorption related to redistribution of charge as a result of secondary doping.^{11,17,27}

The changes in the conductivity (Figure 1), Raman spectra (Figure 2), and AFM images (Figure 3) reported here (as well as the wide-angle X-ray scattering data reported by others¹⁵) are found to be incremental when going from pristine to cosolvent-added to post-treated films. In contrast, UV–vis and EQE results for the post-treated films are discernibly different from those of both pristine and cosolvent-added films.

Compared to the pristine and cosolvent-added films, the post-treated films have been subjected to an additional cycle of swelling and rinsing with the MeOH-EG mixture followed by curing treatment at 110 °C. Such a treatment is known to aid in the segregation and removal of PSS. The result is a higher composition ratio of PEDOT to PSS chains in the post-treated films compared to those of the pristine and cosolvent-added films. This higher density of PEDOT chains leads to the higher absorbance in the visible range.

The higher PCE found for the HSCs with the post-treated films is due to the higher V_{OC} and FF. The dismal performance of the pristine films follows from the poor J_{SC} and FF (Figure 4) and is the result of light-induced structural changes.³² Kinks and imperfections that are more prevalent in the pristine films cause changes in the conjugation and the amount of free radicals, and impede hole transport.³² This is consistent with the higher J_{SC} value found in the EQE measurements (Figure 5) because of the significantly lower light intensity used (1 mW/cm²) when compared to those employed in standard IV measurements (100 mW/cm²).

Overall, the HSCs with the post-treated films show a higher average PCE with the maximum recorded being as high as 11.5%. While the so-called champion-data cells, i.e., those with the best performance, can be achieved, the HSCs with the post-treated films reported here represent a statistical analysis of “production-ready” cells.

CONCLUSION

We developed a novel method of secondary doping for improving PEDOT:PSS in HSCs by using a post-treatment method that employs, for the first time, a 1:1 MeOH:EG binary mixture to remove PSS from the film and hence increase the conductivity. We construct three large sets of cells with PEDOT:PSS films that exhibit vastly different conductivities: pristine (0.8 S/cm), cosolvent-added (637 S/cm), and post-treated films (1334 S/cm). With over a 10% gain in the conductivity obtained for post-treatment with the present binary mixture when compared to that gained for single-solvent post-treatment, post-treatment with a binary mixture offers an improved method for enhancing the conductivity. In addition to the increase in the conductivity, the post-treatment also results in higher V_{OC} through greater interface interaction and charge transfer at the junction, offsetting the decrease in J_{SC} and ultimately increasing the PCE. This work shows a delicate balance when employing PEDOT:PSS for optoelectronic devices and other applications and that gains in conductivity should not come at the expense of other properties such as absorbance.

ASSOCIATED CONTENT

Supporting Information

The Supporting Information is available free of charge on the ACS Publications website at DOI: 10.1021/acsami.6b09704.

Solution properties of methanol ethylene glycol and the mixtures, absorbance of the PEDOT:PSS bands at 193 and 225 nm, and current density vs voltage curves for hybrid solar cells with the maximum efficiencies (PDF)

AUTHOR INFORMATION

Corresponding Author

*E-mail: tong@uwaterloo.ca.

ORCID[®]

K. T. Leung: 0000-0002-1879-2806

Notes

The authors declare no competing financial interest.

ACKNOWLEDGMENTS

This work was supported by the Natural Sciences and Engineering Research Council of Canada.

REFERENCES

- (1) Wright, M.; Uddin, A. Organic-Inorganic Hybrid Solar Cells: A Comparative Review. *Sol. Energy Mater. Sol. Cells* **2012**, *107*, 87–111.
- (2) Weickert, J.; Auras, F.; Bein, T.; Schmidt-Mende, L. Characterisation of Interfacial Modifiers for Hybrid Solar Cells. *J. Phys. Chem. C* **2011**, *115* (30), 15081–15088.
- (3) Gregg, B. A.; Hanna, M. C. Comparing Organic to Inorganic Photovoltaic Cells: Theory, Experiment, and Simulation. *J. Appl. Phys.* **2003**, *93* (6), 3605–3614.
- (4) Yu, P.; Tsai, C.; Chang, J.-K.; Lai, C.-C.; Chen, P.-H.; Lai, Y.-C.; Tsai, P.-T.; Li, M.-C.; Pan, H.-T.; Huang, Y.-Y.; Wu, C.-I.; Chueh, Y.-L.; Chen, S.-W.; Du, C.-H.; Horng, S.-F.; Meng, H.-F. 13% Efficiency Hybrid Organic/Silicon-Nanowire Heterojunction Solar Cell via Interface Engineering. *ACS Nano* **2013**, *7* (12), 10780–10787.
- (5) Nagamatsu, K. A.; Avasthi, S.; Jhaveri, J.; Sturm, J. C. A 12% Efficient Silicon/PEDOT:PSS Heterojunction Solar Cell Fabricated at < 100 °C. *IEEE J. Photovoltaics* **2014**, *4* (1), 260–264.
- (6) Wei, W. R.; Tsai, M. L.; Ho, S.; Tai, S. H.; Ho, C. R.; Tsai, S. H.; Liu, C. W.; Chung, R. J.; He, J. H. Above-11%-Efficiency Organic-Inorganic Hybrid Solar Cells with Omnidirectional Harvesting Characteristics by Employing Hierarchical Photon-Trapping Structures. *Nano Lett.* **2013**, *13* (8), 3658–3663.
- (7) Pudasaini, P. R.; Sharma, M.; Ruiz-Zepeda, F.; Ayon, A. A. Efficiency Improvement of a Nanostructured Polymer Solar Cell Employing Atomic Layer Deposited Al₂O₃ as a Passivation Layer. *Microelectron. Eng.* **2014**, *119*, 6–10.
- (8) Chi, D.; Qi, B.; Wang, J.; Qu, S.; Wang, Z. High-Performance Hybrid Organic-Inorganic Solar Cell Based on Planar N-Type Silicon. *Appl. Phys. Lett.* **2014**, *104* (19), 193903.
- (9) Wu, S.; Cui, W.; Aghdassi, N.; Song, T.; Duhm, S.; Lee, S. T.; Sun, B. Nanostructured Si/Organic Heterojunction Solar Cells with High Open-Circuit Voltage via Improving Junction Quality. *Adv. Funct. Mater.* **2016**, *26* (28), 5035–5041.
- (10) Liu, Y.; Zhang, Z.-G.; Xia, Z.; Zhang, J.; Liu, Y.; Liang, F.; Li, Y.; Song, T.; Yu, X.; Lee, S.-T.; Sun, B. High Performance Nanostructured Silicon-Organic Quasi P-N Junction Solar Cells via Low-Temperature Deposited Hole and Electron Selective Layer. *ACS Nano* **2016**, *10* (1), 704–712.
- (11) Pietsch, M.; Bashouti, M. Y.; Christiansen, S. The Role of Hole Transport in Hybrid Inorganic/Organic Silicon/Poly(3,4-Ethylenedioxythiophene):Poly(styrenesulfonate) Heterojunction Solar Cells. *J. Phys. Chem. C* **2013**, *117* (18), 9049–9055.
- (12) Kim, J. Y.; Jung, J. H.; Lee, D. E.; Joo, J. Enhancement of Electrical Conductivity of poly(3,4-ethylenedioxythiophene)poly(4-Styrenesulfonate) by a Change of Solvents. *Synth. Met.* **2002**, *126*, 311–316.
- (13) Ouyang, J.; Xu, Q.; Chu, C. W.; Yang, Y.; Li, G.; Shinar, J. On the Mechanism of Conductivity Enhancement in poly(3,4-Ethylenedioxythiophene):poly(styrene Sulfonate) Film through Solvent Treatment. *Polymer* **2004**, *45* (25), 8443–8450.
- (14) Crispin, X.; Marciniak, S.; Osikowicz, W.; Zotti, G.; Van Der Gon, A. W. D.; Louwet, F.; Fahlman, M.; Groenendaal, L.; De Schryver, F.; Salaneck, W. R. Conductivity, Morphology, Interfacial Chemistry, and Stability of Poly(3,4-Ethylene Dioxothiophene)-Poly(Styrene Sulfonate): A Photoelectron Spectroscopy Study. *J. Polym. Sci., Part B: Polym. Phys.* **2003**, *41* (21), 2561–2583.
- (15) Takano, T.; Masunaga, H.; Fujiwara, A.; Okuzaki, H.; Sasaki, T. PEDOT Nanocrystal in Highly Conductive PEDOT:PSS Polymer Films. *Macromolecules* **2012**, *45*, 3859–3865.
- (16) Liu, Q.; Imamura, T.; Hiata, T.; Khatri, I.; Tang, Z.; Ishikawa, R.; Ueno, K.; Shirai, H. Optical Anisotropy in Solvent-Modified poly(3,4-Ethylenedioxythiophene): Poly(styrenesulfonic Acid) and Its Effect on the Photovoltaic Performance of Crystalline Silicon/organic Heterojunction Solar Cells. *Appl. Phys. Lett.* **2013**, *102* (24), 243902.
- (17) Pettersson, L. A.; Ghosh, S.; Inganäs, O. Optical Anisotropy in Thin Films of poly(3,4-ethylenedioxythiophene)-poly(4-Styrenesulfonate). *Org. Electron.* **2002**, *3* (3–4), 143–148.
- (18) Thomas, J. P.; Zhao, L.; McGillivray, D.; Leung, K. T. High-Efficiency Hybrid Solar Cells by Nanostructural Modification in PEDOT:PSS with Co-Solvent Addition. *J. Mater. Chem. A* **2014**, *2* (7), 2383–2389.
- (19) Xia, Y.; Ouyang, J. PEDOT:PSS Films with Significantly Enhanced Conductivities Induced by Preferential Solvation with Cosolvents and Their Application in Polymer Photovoltaic Cells. *J. Mater. Chem.* **2011**, *21* (13), 4927–4936.
- (20) Kim, Y. H.; Sachse, C.; Machala, M. L.; May, C.; Müller-Meskamp, L.; Leo, K. Highly Conductive PEDOT:PSS Electrode with Optimized Solvent and Thermal Post-Treatment for ITO-Free Organic Solar Cells. *Adv. Funct. Mater.* **2011**, *21* (6), 1076–1081.
- (21) Alemu, D.; Wei, H.-Y.; Ho, K.-C.; Chu, C.-W. Highly Conductive PEDOT:PSS Electrode by Simple Film Treatment with Methanol for ITO-Free Polymer Solar Cells. *Energy Environ. Sci.* **2012**, *5* (11), 9662–9671.
- (22) Ouyang, J. “Secondary Doping” methods to Significantly Enhance the Conductivity of PEDOT:PSS for Its Application as Transparent Electrode of Optoelectronic Devices. *Displays* **2013**, *34* (5), 423–436.
- (23) Thomas, J. P.; Leung, K. T. Defect-Minimized PEDOT:PSS/planar-Si Solar Cell with Very High Efficiency. *Adv. Funct. Mater.* **2014**, *24* (31), 4978–4985.
- (24) Guo, S.; Solares, S. D.; Mochalin, V.; Neitzel, I.; Gogotsi, Y.; Kalinin, S. V.; Jesse, S. Multifrequency Imaging in the Intermittent Contact Mode of Atomic Force Microscopy: Beyond Phase Imaging. *Small* **2012**, *8* (8), 1264–1269.
- (25) Garreau, S.; Louarn, G.; Buisson, J. In Situ Spectroelectrochemical Raman Studies of Poly(3,4-ethylenedioxythiophene) (PEDT). *Macromolecules* **1999**, *32* (20), 6807–6812.
- (26) Farah, A.; Rutledge, S.; Schaarschmidt, A.; Lai, R.; Freedman, J. P.; Helmy, A. S. Conductivity Enhancement of poly(3,4-Ethylenedioxythiophene)-Poly(styrenesulfonate) Films Post-Spincasting. *J. Appl. Phys.* **2012**, *112* (11), 113709.
- (27) Greczynski, G.; Kugler, T.; Keil, M.; Osikowicz, W.; Fahlman, M.; Salaneck, W. R. Photoelectron Spectroscopy of Thin Films of PEDOT – PSS Conjugated Polymer Blend: A Mini-Review and Some New Results. *J. Electron Spectrosc. Relat. Phenom.* **2001**, *121*, 1–17.
- (28) Nardes, A. M.; Janssen, R. J.; Kemerink, M. A Morphological Model for the Solvent-Enhanced Conductivity of PEDOT:PSS Thin Films. *Adv. Funct. Mater.* **2008**, *18* (6), 865–871.
- (29) Tsierekos, N. G.; Molinou, I. E. Densities and Viscosities of Ethylene Glycol Binary Mixtures at 293.15 K. *J. Chem. Eng. Data* **1999**, *44*, 955–958.
- (30) Lee, I.; Kang, C. H.; Lee, B.-S.; Lee, H. W. Thermodynamic Studies on the Structure of Iso-Dielectric Binary Mixtures of Methanol with Ethylene Glycol, Acetonitrile, Nitrobenzene and Nitromethane. *J. Chem. Soc., Faraday Trans.* **1990**, *86* (9), 1477–1481.
- (31) Cratin, P. D.; Gladden, J. K. Excess Thermodynamic Properties of Binary Liquid System Ethylene Glycol-Methanol. *J. Phys. Chem.* **1963**, *67* (8), 1665–1669.
- (32) Thomas, J. P.; Srivastava, S.; Zhao, L.; Abd-Ellah, M.; McGillivray, D.; Kang, J. S.; Rahman, M. A.; Moghimi, N.; Heinig, N. F.; Leung, K. T. Reversible Structural Transformation and Enhanced Performance of PEDOT:PSS-Based Hybrid Solar Cells Driven by Light Intensity. *ACS Appl. Mater. Interfaces* **2015**, *7*, 7466–7470.
- (33) Kirchartz, T.; Ding, K.; Rau, U. *Advanced Characterization Techniques for Thin Film Solar Cells*; Abou-Ras, D., Kirchartz, T., Rau, U., Eds.; Wiley-VCH Verlag GmbH & Co. KGaA: Weinheim, Germany, 2011.

(34) Dennler, G.; Forberich, K.; Scharber, M. C.; Brabec, C. J.; Tomiš, I.; Hingerl, K.; Fromherz, T. Angle Dependence of External and Internal Quantum Efficiencies in Bulk-Heterojunction Organic Solar Cells. *J. Appl. Phys.* **2007**, *102* (5), 054516.